### Title

Olaparib-Induced Senescence Is Bypassed through G2-M Checkpoint Override in Olaparib-Resistant Prostate Cancer.




### Journal

Molecular cancer therapeutics, 21(4)

### ISSN

1535-7163



### Authors

Lombard, Alan P
Armstrong, Cameron M
D'Abronzo, Leandro S
et al.



### Publication Date

2022-04-01

### DOI

10.1158/1535-7163.mct-21-0604

Peer reviewed

HHS Public Access

Author manuscript

*Mol Cancer Ther*. Author manuscript; available in PMC 2022 October 01.

Published in final edited form as:

*Mol Cancer Ther*. 2022 April 01; 21(4): 677–685. doi:10.1158/1535-7163.MCT-21-0604.

# Olaparib Induced Senescence is Bypassed through G2/M Checkpoint Override in Olaparib Resistant Prostate Cancer

**Alan P Lombard**[1], **Cameron M Armstrong**[1], **Leandro S D'Abronzo**[1], **Shu Ning**[1], **Amy R Leslie**[1], **Masuda Sharifi**[1], **Wei Lou**[1], **Christopher P Evans**[1,2], **Marc Dall'Era**[1,2], **Hong-Wu Chen**[2,3,5], **Xinbin Chen**[2,4], **Allen C Gao**[1,2,5]

[1]Department of Urologic Surgery, University of California Davis, CA, USA

[2]UC Davis Comprehensive Cancer Center, University of California Davis, CA, USA

[3]Department of Biochemistry and Molecular Medicine, University of California Davis, CA, USA

[4]School of Veterinary Medicine, University of California Davis, CA, USA

[5]VA Northern California Health Care System, Sacramento, CA, USA

## Abstract

PARP inhibition represents the dawn of precision medicine for treating prostate cancer. Despite this advance, questions remain regarding the use of PARP inhibitors (PARPi's) for the treatment of this disease, including 1) how specifically do PARPi sensitive tumor cells respond to treatment, and 2) how does PARPi resistance develop? To address these questions, we characterized response to olaparib in sensitive LNCaP and C4–2B cells and developed two olaparib resistant derivative cell line models from each, termed LN-OlapR and 2B-OlapR respectively. OlapR cells possess distinct morphology from parental cells and display robust resistance to olaparib and other clinically relevant PARPi's including rucaparib, niraparib, and talazoparib. In LNCaP and C4–2B cells, we found that olaparib induces massive DNA damage, leading to activation of the G2/M checkpoint, activation of p53, and cell cycle arrest. Furthermore, our data suggest that G2/M checkpoint activation leads to both cell death and senescence associated with p21 activity. In contrast, both LN-OlapR and 2B-OlapR cells do not arrest at G2/M and display a markedly blunted response to olaparib treatment. Interestingly, both OlapR cell lines harbor increased DNA damage relative to parental cells, suggesting that OlapR cells accumulate and manage persistent DNA damage during acquisition of resistance, likely through augmenting DNA repair capacity. Further impairing DNA repair through CDK1 inhibition enhances DNA damage, induces cell death, and sensitizes OlapR cells to olaparib treatment. Our data together further our understanding of PARPi treatment and provide a cellular platform system for the study of response and resistance to PARP inhibition.

### Keywords

PARP; olaparib; prostate cancer; resistance; senescence; G2/M checkpoint

**Corresponding Author:** Allen Gao, University of California Davis, 4645 2nd Avenue, Sacramento, CA 95817, USA. Phone: 916-734-8718, acgao@ucdavis.edu.

Conflict of Interest: None

## Introduction

Treatment of advanced prostate cancer remains challenging due to a paucity of durable therapeutic options. Inhibition of poly (ADP)-ribose polymerase (PARP) has recently emerged as an exciting new treatment strategy for biomarker selected cancer patients (1). PARP is responsible for mediating repair of single strand DNA breaks. Inhibition of PARP is thought to cause unrepaired single strand breaks to lead to increased double strand breaks which must be repaired using other mechanisms such as homologous recombination. It has also been shown that PARP inhibition can cause PARP to become “trapped” at sites of DNA damage, ultimately resulting in DNA breaks (2). In those tumors which harbor defects in certain DNA repair genes, such as BRCA1 and BRCA2, PARP inhibition is hypothesized to cause undue cellular stress leading to cell death in a synthetic lethal manner. In 2005, both Farmer et al and Bryant et al independently determined that tumors deficient in homologous recombination are especially susceptible to PARP inhibition (3,4). Since then, PARP inhibitors (PARPi) have been further studied and developed to translate this exciting and specific treatment strategy to the clinic.

Several trials have demonstrated the efficacy of PARPi’s for the treatment of metastatic castration resistant prostate cancer (mCRPC). The TOPARP-A phase 2 clinical trial demonstrated that PARP inhibition using olaparib appeared efficacious in a subset of mCRPC patients, the majority of which (14 of 16 responders) harbored mutations in DNA repair genes such as BRCA2 (5). These results were confirmed in the phase 2 TOPARP-B study which aimed to test olaparib in prospectively chosen mCRPC patients harboring DNA damage response gene defects (6). The phase 3 PROfound trial demonstrated that patients harboring DNA damage repair defects (most notably BRCA1, BRCA2, and ATM) receiving olaparib fared better than those on investigators choice of either enzalutamide or abiraterone (7,8). The TRITON2 study demonstrated that rucaparib has significant antitumor activity in mCRPC patients with a BRCA deleterious alteration (9). In May 2020, both the PARPi’s rucaparib and olaparib were approved for the treatment of biomarker selected mCRPC patients, representing the dawn of synthetic lethal, precision medicine approaches for the management of this disease. Additional PARPi’s in clinical development for prostate cancer include niraparib and talazoparib (10). However, it should be noted that biomarkers for optimal patient selection for treatment with a PARPi remain poorly understood.

Despite the promise of PARP inhibition for enhancing clinical management of prostate cancer patients, several key questions remain to be answered to optimize their utility including 1) how specifically do PARPi sensitive tumor cells respond to treatment, and 2) how does PARPi resistance develop? It is thought that PARPi’s induce excessive DNA damage in tumor cells ill-equipped to repair double strand breaks, leading to cell death. However, a full understanding of PARPi mechanism of action remains lacking. The signaling cascades which mediate response are not well understood and whether there are alternative responses to treatment is unknown. A better understanding of how PARPi’s function promises to enhance their clinical utility.

The development of therapeutic resistance appears inevitable with treatments used for late-stage prostate cancer. Already, PARPi resistance has been clinically documented in prostate cancer patients with contributing mechanisms appearing to include 1) reversion mutations which replace lost function of defective DNA repair genes and possibly 2) the emergence of a neuroendocrine phenotype (11–13). Basic research studies have also determined additional possible mechanisms of resistance which may include overexpression of the drug efflux transporter ABCB1 and overexpression of PLK1 (14–16). Understanding the development of clinical PARPi resistance will greatly augment the use of PARPi drugs through 1) prolonging their utility, and 2) helping to aid stratification of patients most likely to respond to treatment. Clinically relevant model systems for the study of PARPi response and resistance are needed to aid efforts to address critical, unanswered questions.

In the current study, we introduce two cell line models of olaparib resistance derived from LNCaP cells and its castration-resistant derivative cell line, C4–2B. Olaparib resistant, OlapR, cell lines are shown to be highly insensitive to olaparib and other clinically relevant PARPi's when compared to respective parental control cells. Interrogation of response to treatment in sensitive, parental cells shows that olaparib induces massive DNA damage which elicits a potent p21-mediated G2/M arrest accompanied by both apoptosis and senescence. Interestingly, OlapR cells exhibit a blunted response to treatment which can be overcome through combination treatment with a CDK1 inhibitor. Our study establishes a cell line platform system to further study both response to treatment and the development of resistance.

## Materials and Methods

### Cell culture, reagents, and equipment

C4–2B cells were kindly provided and authenticated by Dr. Leland Chung (Cedars-Sinai Medical Center, Los Angeles, CA). LNCaP, Rv1, and PC3 cells were obtained from the American Type Culture Collection (ATCC). ATCC uses short tandem repeat profiling for testing and authentication of cell lines. All cell lines are routinely tested for mycoplasma using ABM mycoplasma PCR detection kit (Cat#: G238). All experiments with these cell lines and their derivatives were conducted within 6 months of receipt or resuscitation after cryopreservation. LNCaP, C4–2B, Rv1, and PC3 cells were maintained in RPMI 1640 media supplemented with 10% fetal bovine serum, 100 IU penicillin and 0.1 mg/ml streptomycin. Olaparib-resistant LN-OlapR and 2B-OlapR cells were derived from LNCaP and C4–2B cells respectively through chronic exposure to increasing doses of olaparib for over 1 year. Both OlapR cell lines are maintained in complete RPMI 1640 supplemented with 5μM olaparib. LNCaP and C4–2B cells were cultured alongside OlapR derivative cell lines as appropriate controls. All cells were maintained at 37°C in a humidified incubator with 5% carbon dioxide. Olaparib (Cat#: S1060), niraparib (Cat#: S2741), talazoparib (Cat#: S7048), and BMS-265246 (Cat#: S2014) were purchased from Selleckchem (17). Rucaparib (Cat#: 6230/10) was purchased from R&D Systems. RNAi was performed using Dicer-Substrate siRNAs (DsiRNA) purchased from IDT. The following DsiRNA's were used; Negative Control (NC) = Cat#: 51–01-14–04, p21 = Cat#: hs.Ri.CDKN1A.13.1, CDK1 = Cat#: hs.Ri.CDK1.13.1. Transfection of DsiRNA's was done using Lipofectamine RNAiMAX

(Cat#: 56532) purchased from ThermoFisher Scientific according to manufacturer's protocol with 25 or 50nM DsiRNA. Microscopy was performed using a Keyence BZ-X810 imaging system.

### Cell growth assays

Cells were plated at a density of 10,000–40,000 cells/well in 24-well plates in complete media without any selection agent. After 24 hours, cells were subjected to indicated treatments. For experiments combining RNAi with drug, transfection of DsiRNA was performed 24 hours after plating and drug was administered as indicated the following day. Cell viability was assessed 72–120 hours post drug treatment using Cell Counting Kit-8 (Cat#: CK04–20) purchased from Dojindo Molecular Technologies, Inc. Alternatively, cells were counted via Coulter Particle Counter. Data is displayed as percent of control cell growth ± standard deviation. All conditions were performed in triplicate or quadruplicate.

### Preparation of Whole Cell Lysates

Cells were harvested, washed with PBS, and lysed in RIPA buffer supplemented with 5mM EDTA, 1mM NaV, 10mM NaF, and 1X Halt Protease Inhibitor Cocktail (Cat#: 78430) purchased from ThermoFisher. Protein concentration was determined with Pierce Coomassie Plus (Bradford) Assay Kit (Cat#: 23236) purchased from ThermoFisher.

### Western Blot

Protein extracts were resolved by SDS-PAGE and indicated primary antibodies were used; PARP (Cat# 9532, rabbit-monoclonal, 1:1000 dilution), yH2AX (Cat# 9718, rabbit-monoclonal, 1:1000 dilution), phospho-p53 Ser15 (Cat# 9284, rabbit-polyclonal, 1:1000 dilution), Bax (Cat# 2772, rabbit-polyclonal, 1:1000 dilution), cleaved-PARP (Cat# 9541, rabbit-polyclonal, 1:1000 dilution), and CDK1 (Cat# 9116, mouse-monoclonal, 1:1000 dilution) were purchased from Cell Signaling Technology. PAR (Cat#: 4336-BPC-100, rabbit-polyclonal, 1:1000 dilution) was purchased from Trevigen. p21 (Cat# SC-397, rabbit-polyclonal, 1:1000 dilution) and Actin (Cat# SC-1616, goat-polyclonal, 1:1000 dilution) were purchased from Santa Cruz Biotechnology. Tubulin (T5168, mouse-monoclonal, 1:6000 dilution) was purchased from Sigma-Aldrich. Tubulin or Actin were used to monitor the amounts of samples applied. Proteins were visualized with a chemiluminescence detection system (Cat#: WBLUR0500) purchased from Millipore.

### Flow Cytometry

Cell cycle distribution was determined by propidium iodide staining analysis using a GUAVA MUSE cell analyzer flow cytometer (Luminex). Propidium iodide stain (Cat#: ab139418) was purchased from Abcam and staining was done following manufacturers protocol. Briefly, cells were treated as indicated for 5 days followed by harvest, wash, and fixed overnight in 66% EtOH at 4C. Cells were washed the following day and stained with propidium iodide staining solution containing 100ug/ml RNase A and subsequently run and analyzed via GUAVA MUSE. Data is displayed as percent of cells in each phase ± standard deviation. All conditions were performed in triplicate.

### Beta-Galactosidase Activity Assay

Beta-galactosidase activity was assessed using staining kit (Cat#: 9860S) purchased from Cell Signaling Technology using manufacturers protocol. Briefly, cells were treated as indicated for 5 days, washed, fixed, and stained overnight in a dry, 37°C incubator. Stained cells were subsequently imaged the following day and images were used for quantification via percent of positively stained cells in several fields per image. Data is displayed as an average percent of positively stained cells per field ± standard deviation.

### Statistics

Significance was assessed using a two tailed two sample equal variance students t-test. A p-value ≤ 0.05 was accepted as significant. All experiments were performed at least twice.

### Data Availability

The data generated in this study are available within the article.

## Results

### Development of LNCaP and C4–2B based models of acquired olaparib resistance

We began our study by determining response to olaparib in various cell line models of prostate cancer. We found that the castration-sensitive cell line, LNCaP, and its castration-resistant cell line derivative, C4–2B, exhibited a stronger response to olaparib than other tested cells (Fig. 1A). A previous study showed that LNCaP harbors a BRCA2 mutation likely to confer sensitivity to PARP inhibition making it and its derivative, C4–2B, attractive models for the study of PARPi sensitivity (18). To study olaparib resistance, we subjected both LNCaP and C4–2B cells to chronic exposure of increasing doses of olaparib over an ~1-year period (Fig. 1B). This resulted in the development of two, novel olaparib resistant cell line derivatives, LN-OlapR from LNCaP cells and 2B-OlapR from C4–2B cells. Cell growth assays demonstrate that each OlapR cell line exhibits robust resistance to olaparib versus parental, olaparib sensitive cell lines (Fig. 1C). Respective $IC_{50}$ values for each are as follows; (LNCaP = 6μM, LN-OlapR = 18μM, C4–2B = 3μM, 2B-OlapR = 106μM). Imaging of each cell line reveals clear morphological differences in OlapR cells versus parental cells indicating robust alterations to cellular phenotype (Fig. 1D). Notably, both OlapR cell lines appear more rounded than corresponding parental cell lines.

### OlapR cells are cross-resistant to other clinically relevant PARP inhibitors

As previously noted, additional PARPi's are either approved or are undergoing clinical testing for the treatment of prostate cancer, including rucaparib, niraparib, and talazoparib. However, each PARPi has a unique structure and possesses varying abilities to both inhibit PARP catalytic activity and trap PARP onto DNA (2,19). Whether resistance to olaparib induces PARPi cross-resistance is not known but may have important research and clinical implications. Interestingly, cell growth assays demonstrate that each OlapR cell line exhibits cross-resistance to other clinically relevant PARPi's, including rucaparib, niraparib, and talazoparib (Fig. 2). These data suggest that OlapR cells represent useful models of pan-

PARPi resistance and that it is likely that mechanisms which confer resistance to olaparib may confer resistance to other PARPi's.

## OlapR olaparib resistance is characterized by G2/M checkpoint override

We sought to better characterize resistance in OlapR cells. PARP1 is the most abundant member of the PARP family and accounts for ~90% of PARylation activity (20,21). We first asked whether altered PARP1 expression may be involved in the development of resistance. Western blots revealed no difference in PARP1 expression in OlapR cells versus control cells (Fig. 3A). We next tested whether altered PARP activity plays a role. We performed western blots for PAR to assess olaparib's ability to inhibit PARP catalytic function in OlapR and parental cells. Western blots show that after 5-day olaparib treatment, PARylation is significantly inhibited in both OlapR and parental cells (Fig. 3B), suggesting that resistance is not dependent upon alteration to olaparib's ability to inhibit PARylation.

It is thought that PARPi's induce DNA damage and subsequent death in cells harboring DNA repair defects. Western blots reveal a dramatic increase in yH2AX levels, a marker for double strand DNA breaks, in olaparib treated LNCaP and C4–2B cells (Fig. 3B). This is consistent with the currently accepted mechanism of action of olaparib. However, in OlapR cells, there is no increase in yH2AX levels when treated with olaparib (Fig. 3B). Interestingly, we do note that untreated, both OlapR cell lines possess increased yH2AX expression relative to parental cells. These data suggest that OlapR cells do not accumulate DNA damage in response to olaparib treatment, unlike sensitive parental LNCaP and C4–2B cells. However, PARPi resistant cells appear to retain and manage a high level of residual DNA damage from chronic treatment.

Our data suggest that resistance to olaparib is not dependent on altered PARP expression or on inhibition of PARPi function, but rather downstream response to treatment. Our data further supports that olaparib induces DNA damage in sensitive cells, but not OlapR cells, although OlapR cells appear to manage high levels of residual DNA damage accumulated during resistance acquisition. To further characterize response to PARP inhibition, we performed flow cytometry to assess cell cycle distribution in response to olaparib. We found that treatment induces a robust G2/M arrest in both LNCaP and C4–2B cells, suggestive of G2/M cell cycle checkpoint activation in response to induced DNA damage (Fig. 3C). However, in both OlapR models, we found no G2/M arrest in response to treatment, suggesting resolution of G2/M checkpoint activation in these cells. Altogether, our data suggest that olaparib induces a robust G2/M arrest in sensitive LNCaP and C4–2B cells, but that OlapR cells evade PARPi response via override of G2/M checkpoint activation, allowing for cell survival and management of high levels of residual DNA damage.

## Olaparib induces both apoptosis and senescence

The G2/M checkpoint can be activated and mediated by several well characterized cascades which may include activation of p53 and downstream signaling. Western blots show that olaparib treated LNCaP and C4–2B cells display increased levels of Ser15 phosphorylated p53, indicating activation (Fig. 3D). Furthermore, we found increased levels of the pro-apoptotic, p53-target BAX and cleaved-PARP, suggesting induction of cell death (Fig. 3D)

(22–24). We found comparatively less p53 activation in OlapR cells and an absent or blunted apoptotic response. These data suggest that p53 signaling and upstream signal activation is blunted in OlapR cells in response to PARPi induced DNA damage.

Close visual observation of olaparib treated LNCaP and C4–2B cells suggested that while some cells undergo apoptosis, a significant population of cells appear to display a cytostatic response with an altered morphology (Fig. 4A). In contrast, we did not observe significantly altered morphology in olaparib treated OlapR cells. We hypothesized that PARPi treatment may induce G2/M arrested senescence, which could have important clinical implications. To characterize this phenotype, we performed beta-galactosidase activity assays (Fig. 4B). Staining for increased beta-galactosidase activity, a hallmark of senescent cells, indicates that olaparib treatment induces senescence in LNCaP and C4–2B cells, but to a much lesser extent in OlapR cells. Together, our results imply that 1) PARP inhibition induces G2/M checkpoint activation resulting in increased p53 signaling leading to both cell death and senescence and 2) PARPi acquired resistance is mediated by G2/M checkpoint override.

## Olaparib induced senescence is associated with p21 expression

Treatment induced senescence is thought to have important clinical implications. Thus, understanding treatment induced senescence and the mechanisms responsible for this phenotype is key in better utilizing certain drugs. Senescence is thought to be maintained largely through the activity of cyclin dependent kinase inhibitors such as p21 (25,26). p21 is a critical target of p53, prompting us to first assess the possibility that olaparib induced senescence is mediated by p21. Indeed, we found increased p21 expression in olaparib treated LNCaP and C4–2B cells, but not in olaparib treated OlapR cells (Fig. 5A).

Senescence may provide some cells an escape from PARPi cytotoxicity through cell cycle arrest. These cells may then be a repository of surviving cells which may later promote treatment resistance (27). We hypothesized that inhibition of p21 would block entry into senescence and promote increased cell death in response to olaparib due to increased DNA damage during cellular proliferation. Western blots show that p21 inhibition causes increased DNA damage in combination with olaparib and marked increases in cleaved-PARP, suggesting robust apoptosis (Fig. 5B). RNAi-mediated inhibition of p21 expression led to enhanced efficacy of olaparib in reducing cellular viability (Fig. 5C). Furthermore, imaging of treated cells suggests increased cell death in lieu of senescence when p21 inhibition is combined with olaparib treatment (Fig. 5D). Our data support that senescence associated with p21 activity is an alternative PARPi response which may provide a repository of surviving cells which escape PARPi cytotoxicity and may give rise to resistant cell populations.

## CDK1 inhibition sensitizes OlapR cells to olaparib treatment

While parental LNCaP and C4–2B cells undergo G2/M checkpoint activation in response to olaparib, resistant OlapR models do not. Interestingly, despite override of the G2/M checkpoint, both LN-OlapR and 2B-OlapR cells appear to have much higher, intrinsic DNA damage versus parental cells, even in the absence of treatment (Fig. 3B). These data suggest that olaparib resistant cells 1) devise means to survive persistent DNA damage and/or 2)

upregulate DNA damage repair mechanisms. A previous report demonstrated that in the context of BRCA-wild type tumor cells (presumably homologous recombination proficient), CDK1 inhibition could impair DNA damage repair and sensitize cells to PARP inhibition, while not sensitizing non-transformed cells (28). While the mechanism which promotes survival despite persistent DNA damage remains to be elucidated, we hypothesized that CDK1 inhibition would impair DNA repair, further augment DNA damage, and sensitize OlapR cells to treatment. Indeed, we found that siRNA-mediated downregulation of CDK1 drastically increased the DNA damage marker yH2AX, as well as cleaved-PARP indicating induction of apoptosis (Fig. 6A). Furthermore, we found that CDK1 knockdown decreased OlapR cell viability and enhanced olaparib efficacy (Fig. 6B). Like RNAi, a CDK1 small molecule inhibitor, BMS-265246 (BMS), also decreased OlapR cell viability, increased DNA damage, induced apoptosis, and sensitized to olaparib (Fig. 6C–E) (17). Altogether, our data suggest that inhibition of CDK1 can impair DNA damage repair in olaparib resistant cells, reduce cellular viability, and enhance olaparib efficacy.

## Discussion

PARP inhibition represents the dawn of precision of medicine for prostate cancer and ushers in an era of new strategies aimed at exploiting synthetic lethality in tumors. The year 2020 saw two PARPi's, olaparib and rucaparib, approved for prostate cancer treatment while additional PARPi's remain in clinical development. This exciting new approach promises to significantly enhance our ability to prolong the lives of men suffering from this disease, but several questions remain to be answered regarding their use, including 1) how specifically PARP inhibitors function, 2) how do PARPi sensitive tumor cells respond to treatment, and 3) how does PARPi resistance develop? In the present study, we characterize PARPi sensitive prostate cancer cell lines and developed olaparib resistant derivative cells (OlapR). OlapR cells are shown to be highly resistant to olaparib and to exhibit marked cross-resistance to other clinically relevant PARPi's, including the approved rucaparib. Interrogation of response to treatment shows that olaparib induces massive DNA damage in sensitive cells which elicits a potent p21-mediated G2/M arrest response accompanied by both apoptosis and senescence. Interestingly, OlapR cells exhibit a blunted response to treatment which can be overcome through combination treatment with a CDK1 inhibitor. It should be noted that a previous study presented data suggesting Rv1 may also harbor deleterious BRCA2 mutation, but not PC3 (18). We hypothesize that uncharacterized mechanisms of resistance render Rv1 less sensitive to treatment. Why LNCaP and C4–2B cells are so much more sensitive is not completely understood, but clearly, additional study is needed to fully elucidate markers of resistance and sensitivity to PARP inhibitors. Our study establishes a cellular platform system to further study both response to treatment and the development of resistance.

Our study showed that OlapR cells are robustly cross-resistant to other PARPi's in prostate cancer clinical development. Thus, OlapR cells can be thought of as pan-PARPi resistant, which could enhance their utility as a research tool. These data suggest that mechanisms of resistance to one PARPi will often induce resistance to the drug-class, which indicates that sequencing additional PARPi's post initial treatment is likely a poor management strategy. Despite this finding, it is known that different PARPi's have distinct structures and varying

strengths and properties (2,19). Most notably, it is known that PARPi's both inhibit PARP catalytic activity and trap PARP at sites of DNA damage. Trapping is thought to be more indicative of anti-tumor activity and different PARPi's exhibit varying abilities to trap PARP, with talazoparib being the strongest (19). Whether different drug properties will eventually lead to an optimal clinical choice remains unknown.

In line with current hypotheses, our data show that olaparib abolishes PARP catalytic activity and induces massive amounts of DNA double strand breaks. Furthermore, we find that olaparib treatment induces a robust G2/M arrest characterized by activation of p53 signaling. While this ultimately leads to increased cell death as expected, we also found a significant proportion of cells evade death and undergo senescence associated with p21 activity. Persistent, PARPi-induced senescent cells could have profound clinical implications. Senescent cells, while no longer able to divide, are known to be highly active and to elicit profound effects on their micro-environments, largely through their acquisition of the senescence-associated secretory phenotype (29,30). These properties are thought to be possibly linked to the promotion of tumor progression and the development of treatment resistance (31). Furthermore, the potential for re-emergence from senescence could allow persistent cells to form a repository of surviving cells which may then go on to proliferate and give rise to recurrent, resistant disease (27). A recent study found that PARPi treatment also induces both cell death and senescence in the context of ovarian and breast cancer (26). This study found that PARP inhibition could induce a p21-dependent senescence which was reversible possibly providing a pathway to recurrent disease. However, their work demonstrated that senescence was independent of p53 and rather relied upon Chk2 activation, highlighting the diverse mechanisms which can be activated in response to these drugs. Fully understanding response to PARP inhibition in each tumor context is imperative toward maximizing PARPi's as a treatment strategy. Inputs leading to activation of p53 in our study remain unknown, but their elucidation could provide novel therapeutic targets for combination with PARP inhibition. It is thought that targeting senescence using senolytic drugs could prove to be an effective form of precision medicine by clearing treatment induced senescent cells thus enhancing treatment efficacy (32). Senescent cells rely upon activation of various pro-survival pathways. Furthermore, senescent cells are highly metabolically active. These specific pathways may provide vulnerabilities which can be exploited for the specific clearing of persistent, senescent cells thus providing a means to greatly increase the utility of a treatment which induces senescence, like olaparib.

Interestingly, there is increased yH2AX in OlapR cells versus control cells, which suggests that while olaparib does not increase DNA damage in resistant cells, OlapR models deal with constant and persistent DNA damage acquired during progression to a resistant state. Despite this drastic increase in persistent damage, OlapR models continue to proliferate and do not exhibit G2/M arrest. These findings imply that PARPi resistant cells must employ mechanisms to manage persistent DNA damage and or mitigate the DNA damage response while increasing survival pathways. While these specific resistance mechanisms remain to be defined, we sought a means to sensitize resistant cells to treatment. A previous study demonstrated that targeting CDK1 could render BRCA-proficient cells sensitive to PARP inhibition through impairment of homologous recombination potential (28). In line with these findings, our data show that inhibition of CDK1 induces DNA damage and cell death

in OlapR cell line models. Furthermore, CDK1 inhibition reduces cellular viability and sensitizes to olaparib treatment. These data provide proof of concept that CDK1 targeting could be developed to overcome acquired resistance to PARP inhibition.

In conclusion, our findings demonstrate that response to olaparib is characterized by increased DNA damage which elicits p53 activation and G2/M arrest. This response leads to both cell death and senescence associated with p21 activity which may be targetable to further augment DNA damage and promote cell death over senescence. PARPi resistant cells appear to override the G2/M checkpoint in response to treatment but resistance may be overcome through further targeting DNA repair via inhibition of CDK1. Data presented here represent a platform for the study of PARP inhibition in prostate cancer which promises to lead to critical insights into the development and mitigation of resistance to this exciting new treatment strategy.

## Financial Support:

This work was supported in part by grants CA179970 (A.C. G), CA 225836 (A.C.G), DOD PC180180 (A.C.G), and the U.S. Department of Veterans Affairs, Office of Research & Development BL&D grant number I01BX004036 (A.C. G), BLR&D Research Career Scientist Award IK6BX005222 (A.C. G). A.C.G is also a Senior Research Career Scientist at VA Northern California Health Care System, Mather, California. NCI K01 1K01CA262351-01 (A.P.L)

## References

1. Nizialek E, Antonarakis ES. PARP Inhibitors in Metastatic Prostate Cancer: Evidence to Date. Cancer Manag Res 2020;12:8105–14 doi 10.2147/CMAR.S227033. [PubMed: 32982407]
2. Murai J, Huang SY, Das BB, Renaud A, Zhang Y, Doroshow JH, et al. Trapping of PARP1 and PARP2 by Clinical PARP Inhibitors. Cancer Res 2012;72(21):5588–99 doi 10.1158/0008-5472.CAN-12-2753. [PubMed: 23118055]
3. Bryant HE, Schultz N, Thomas HD, Parker KM, Flower D, Lopez E, et al. Specific killing of BRCA2-deficient tumours with inhibitors of poly(ADP-ribose) polymerase. Nature 2005;434(7035):913–7 doi 10.1038/nature03443. [PubMed: 15829966]
4. Farmer H, McCabe N, Lord CJ, Tutt AN, Johnson DA, Richardson TB, et al. Targeting the DNA repair defect in BRCA mutant cells as a therapeutic strategy. Nature 2005;434(7035):917–21 doi 10.1038/nature03445. [PubMed: 15829967]
5. Mateo J, Carreira S, Sandhu S, Miranda S, Mossop H, Perez-Lopez R, et al. DNA-Repair Defects and Olaparib in Metastatic Prostate Cancer. N Engl J Med 2015;373(18):1697–708 doi 10.1056/NEJMoa1506859. [PubMed: 26510020]
6. Mateo J, Porta N, Bianchini D, McGovern U, Elliott T, Jones R, et al. Olaparib in patients with metastatic castration-resistant prostate cancer with DNA repair gene aberrations (TOPARP-B): a multicentre, open-label, randomised, phase 2 trial. Lancet Oncol 2020;21(1):162–74 doi 10.1016/S1470-2045(19)30684-9. [PubMed: 31806540]
7. de Bono J, Mateo J, Fizazi K, Saad F, Shore N, Sandhu S, et al. Olaparib for Metastatic Castration-Resistant Prostate Cancer. N Engl J Med 2020;382(22):2091–102 doi 10.1056/NEJMoa1911440. [PubMed: 32343890]
8. Hussain M, Mateo J, Fizazi K, Saad F, Shore N, Sandhu S, et al. Survival with Olaparib in Metastatic Castration-Resistant Prostate Cancer. N Engl J Med 2020;383(24):2345–57 doi 10.1056/NEJMoa2022485. [PubMed: 32955174]
9. Abida W, Patnaik A, Campbell D, Shapiro J, Bryce AH, McDermott R, et al. Rucaparib in Men With Metastatic Castration-Resistant Prostate Cancer Harboring a BRCA1 or BRCA2 Gene Alteration. J Clin Oncol 2020;38(32):3763–72 doi 10.1200/JCO.20.01035. [PubMed: 32795228]

10. Virtanen V, Paunu K, Ahlskog JK, Varnai R, Sipeky C, Sundvall M. PARP Inhibitors in Prostate Cancer-The Preclinical Rationale and Current Clinical Development. Genes (Basel) 2019;10(8) doi 10.3390/genes10080565.
11. Goodall J, Mateo J, Yuan W, Mossop H, Porta N, Miranda S, et al. Circulating Cell-Free DNA to Guide Prostate Cancer Treatment with PARP Inhibition. Cancer Discov 2017;7(9):1006–17 doi 10.1158/2159-8290.CD-17-0261. [PubMed: 28450425]
12. Horak P, Weischenfeldt J, von Amsberg G, Beyer B, Schutte A, Uhrig S, et al. Response to olaparib in a PALB2 germline mutated prostate cancer and genetic events associated with resistance. Cold Spring Harb Mol Case Stud 2019;5(2) doi 10.1101/mcs.a003657.
13. Quigley D, Alumkal JJ, Wyatt AW, Kothari V, Foye A, Lloyd P, et al. Analysis of Circulating Cell-Free DNA Identifies Multiclonal Heterogeneity of BRCA2 Reversion Mutations Associated with Resistance to PARP Inhibitors. Cancer Discov 2017;7(9):999–1005 doi 10.1158/2159-8290.CD-17-0146. [PubMed: 28450426]
14. Lombard AP, Liu C, Armstrong CM, D'Abronzo LS, Lou W, Chen H, et al. Overexpressed ABCB1 Induces Olaparib-Taxane Cross-Resistance in Advanced Prostate Cancer. Transl Oncol 2019;12(7):871–8 doi 10.1016/j.tranon.2019.04.007. [PubMed: 31075528]
15. Li J, Wang R, Kong Y, Broman MM, Carlock C, Chen L, et al. Targeting Plk1 to Enhance Efficacy of Olaparib in Castration-Resistant Prostate Cancer. Mol Cancer Ther 2017;16(3):469–79 doi 10.1158/1535-7163.MCT-16-0361. [PubMed: 28069876]
16. Lombard AP, Gao AC. Resistance Mechanisms to Taxanes and PARP Inhibitors in Advanced Prostate Cancer. Curr Opin Endocr Metab Res 2020;10:16–22 doi 10.1016/j.coemr.2020.02.006. [PubMed: 32258820]
17. Misra RN, Xiao H, Rawlins DB, Shan W, Kellar KA, Mulheron JG, et al. 1H-Pyrazolo[3,4-b]pyridine inhibitors of cyclin-dependent kinases: highly potent 2,6-Difluorophenacyl analogues. Bioorg Med Chem Lett 2003;13(14):2405–8 doi 10.1016/s0960-894x(03)00381-0. [PubMed: 12824044]
18. Feiersinger GE, Trattnig K, Leitner PD, Guggenberger F, Oberhuber A, Peer S, et al. Olaparib is effective in combination with, and as maintenance therapy after, first-line endocrine therapy in prostate cancer cells. Mol Oncol 2018;12(4):561–76 doi 10.1002/1878-0261.12185. [PubMed: 29465803]
19. Murai J, Huang SY, Renaud A, Zhang Y, Ji J, Takeda S, et al. Stereospecific PARP trapping by BMN 673 and comparison with olaparib and rucaparib. Mol Cancer Ther 2014;13(2):433–43 doi 10.1158/1535-7163.MCT-13-0803. [PubMed: 24356813]
20. Burkle A, Diefenbach J, Brabeck C, Beneke S. Ageing and PARP. Pharmacol Res 2005;52(1):93–9 doi 10.1016/j.phrs.2005.02.008. [PubMed: 15911337]
21. Luo X, Kraus WL. On PAR with PARP: cellular stress signaling through poly(ADP-ribose) and PARP-1. Genes Dev 2012;26(5):417–32 doi 10.1101/gad.183509.111. [PubMed: 22391446]
22. Westphal D, Kluck RM, Dewson G. Building blocks of the apoptotic pore: how Bax and Bak are activated and oligomerize during apoptosis. Cell Death Differ 2014;21(2):196–205 doi 10.1038/cdd.2013.139. [PubMed: 24162660]
23. Gao C, Wang AY. Significance of increased apoptosis and Bax expression in human small intestinal adenocarcinoma. J Histochem Cytochem 2009;57(12):1139–48 doi 10.1369/jhc.2009.954446. [PubMed: 19729672]
24. Fridman JS, Lowe SW. Control of apoptosis by p53. Oncogene 2003;22(56):9030–40 doi 10.1038/sj.onc.1207116. [PubMed: 14663481]
25. Coppe JP, Rodier F, Patil CK, Freund A, Desprez PY, Campisi J. Tumor suppressor and aging biomarker p16(INK4a) induces cellular senescence without the associated inflammatory secretory phenotype. J Biol Chem 2011;286(42):36396–403 doi 10.1074/jbc.M111.257071. [PubMed: 21880712]
26. Fleury H, Malaquin N, Tu V, Gilbert S, Martinez A, Olivier MA, et al. Exploiting interconnected synthetic lethal interactions between PARP inhibition and cancer cell reversible senescence. Nat Commun 2019;10(1):2556 doi 10.1038/s41467-019-10460-1. [PubMed: 31186408]
27. Gordon RR, Nelson PS. Cellular senescence and cancer chemotherapy resistance. Drug Resist Updat 2012;15(1–2):123–31 doi 10.1016/j.drup.2012.01.002. [PubMed: 22365330]

28. Johnson N, Li YC, Walton ZE, Cheng KA, Li D, Rodig SJ, et al. Compromised CDK1 activity sensitizes BRCA-proficient cancers to PARP inhibition. Nat Med 2011;17(7):875–82 doi 10.1038/nm.2377. [PubMed: 21706030]

29. Coppe JP, Desprez PY, Krtolica A, Campisi J. The senescence-associated secretory phenotype: the dark side of tumor suppression. Annu Rev Pathol 2010;5:99–118 doi 10.1146/annurev-pathol-121808-102144. [PubMed: 20078217]

30. Faget DV, Ren Q, Stewart SA. Unmasking senescence: context-dependent effects of SASP in cancer. Nat Rev Cancer 2019;19(8):439–53 doi 10.1038/s41568-019-0156-2. [PubMed: 31235879]

31. Chambers CR, Ritchie S, Pereira BA, Timpson P. Overcoming the senescence-associated secretory phenotype (SASP): a complex mechanism of resistance in the treatment of cancer. Mol Oncol 2021 doi 10.1002/1878-0261.13042.

32. Carpenter VJ, Saleh T, Gewirtz DA. Senolytics for Cancer Therapy: Is All That Glitters Really Gold? Cancers (Basel) 2021;13(4) doi 10.3390/cancers13040723.

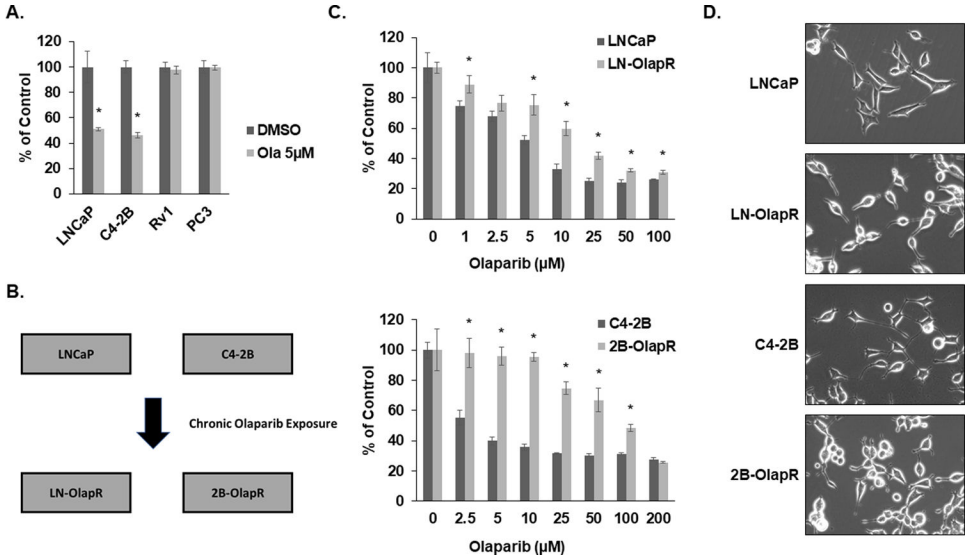


**Figure 1: Development of olaparib resistant LN-OlapR and 2B-OlapR cell line models.**

**A.** Cell viability assay demonstrates olaparib response in indicated prostate cancer cell line models at 72 hours post treatment. **B.** Schematic for creation of OlapR models from parental LNCaP and C4–2B cells. **C.** Cell viability assays demonstrate robust resistance to olaparib in LN-OlapR and 2B-OlapR cells versus respective LNCaP and C4–2B parental cells 72 hours post treatment. **D.** Cell imaging shows distinct morphology of OlapR cells versus parental cells. * = p-value ≤ 0.05 between OlapR and parental cell line.

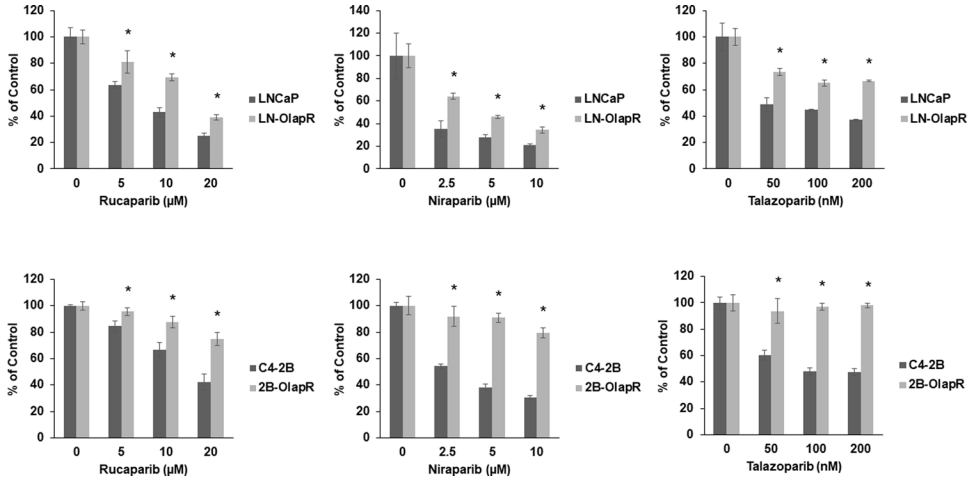


**Figure 2: OlapR cell line models are cross resistant to additional clinically relevant PARP inhibitors.**

Cell viability assays demonstrate that both LN-OlapR and 2B-OlapR are cross-resistant to the additionally tested PARP inhibitors rucaparib, niraparib, and talazoparib versus parental LNCaP and C4–2B cells respectively. Assays were performed 72 hours post treatment. * = p-value ≤ 0.05 between OlapR and parental cell line.

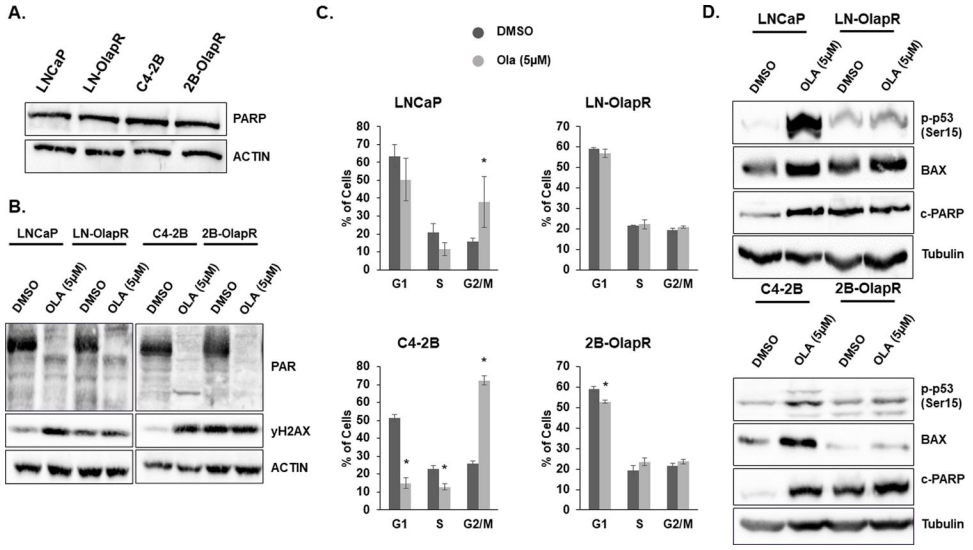


**Figure 3: Olaparib induced G2/M checkpoint activation is blunted in OlapR cells.**

**A.** Whole cell lysates collected 48 hours after plating without selection agent were subjected to western blot for PARP-1. Actin served as a loading control. **B.** Whole cell lysates from indicated cell lines treated with olaparib or vehicle control for 5 days were subjected to western blot analysis for indicated proteins. Actin served as a loading control. **C.** 5-day olaparib treated LNCaP, C4–2B, LN-OlapR, and 2B-OlapR cells were subjected to flow cytometry for cell cycle analysis. **D.** Whole cell lysates from indicated cell lines treated with olaparib or vehicle control for 5 days were subjected to western blot analysis for indicated proteins. Tubulin served as a loading control. * = p-value ≤ 0.05 between OlapR and parental cell line.

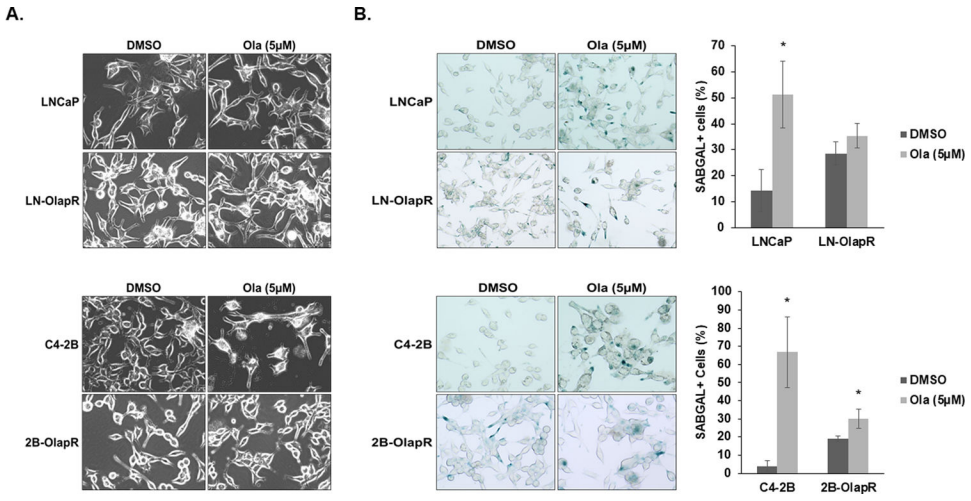


**Figure 4: Olaparib induces senescence morphology and increases beta-galactosidase activity in sensitive cells but not OlapR cells.**

**A.** LNCaP, LN-OlapR, C4–2B, and 2B-OlapR cells were treated with olaparib or vehicle for 5 days and subsequently imaged. **B.** LNCaP, LN-OlapR, C4–2B, and 2B-OlapR cells were treated with olaparib or vehicle for 5 days and subsequently subjected to beta-galactosidase activity assays. * = p-value ≤ 0.05 between OlapR and parental cell line.

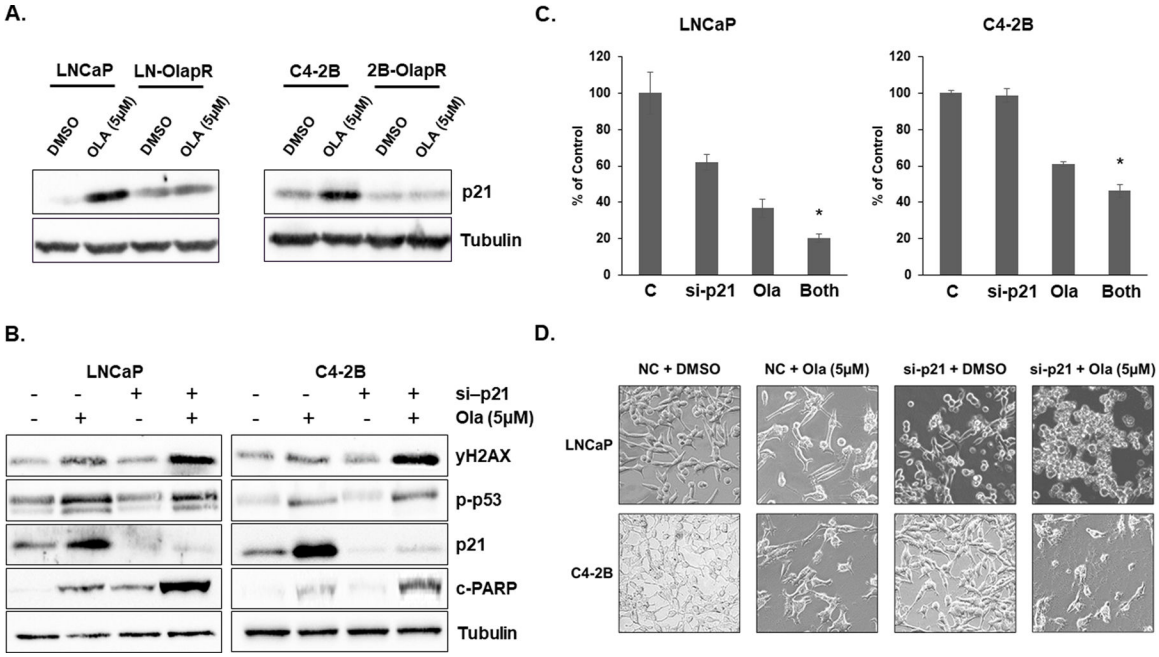


**Figure 5: Olaparib induced senescence is p21 dependent.**

**A.** Whole cell lysates from LNCaP, LN-OlapR, C4–2B, and 2B-OlapR cells treated with olaparib or vehicle for 5 days were subjected to western blot for p21 expression. Tubulin served as a loading control. **B.** LNCaP and C4–2B cells were treated with si-p21 and subsequently treated with 5μM olaparib the following day. Samples were harvested 48 hours post olaparib treatment. Whole cell lysates were subjected to western blot for indicated proteins. Tubulin served as a loading control. **C.** LNCaP and C4–2B cells were treated with si-p21 and subsequently treated with 5μM olaparib the following day. Cell viability was assessed 96 hours post olaparib treatment. **D.** LNCaP and C4–2B cells were treated with si-p21 followed by olaparib the following day. Cells were imaged 96 hours post olaparib treatment. * = p-value ≤ 0.05 compared to all other samples.

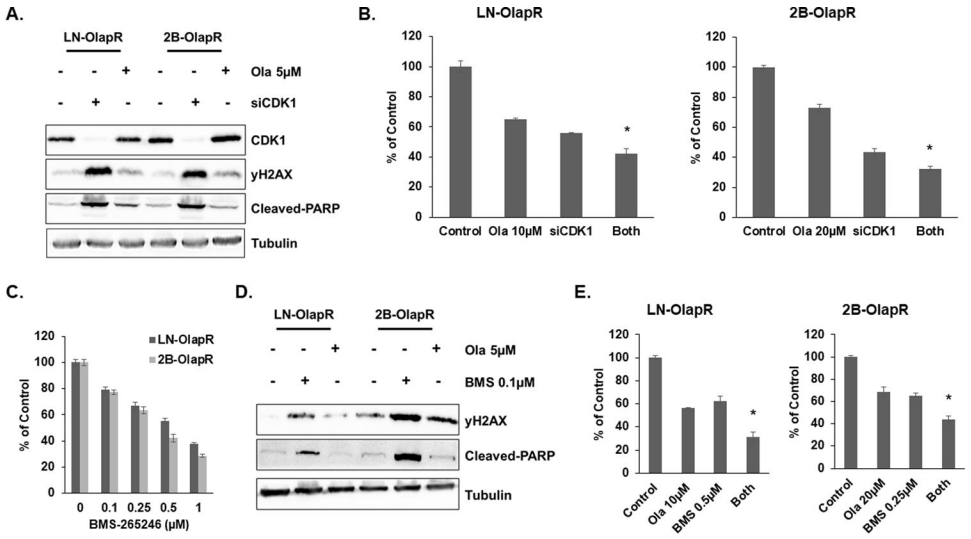


**Figure 6. CDK1 inhibition induces DNA damage and sensitizes resistant cells to olaparib treatment.**

**A.** LN-OlapR and 2B-OlapR cells were treated with either siCDK1 or olaparib for 72 hours. Whole cell lysates were then prepared and subjected to western blot for indicated proteins. Tubulin served as a loading control. **B.** LN-OlapR and 2B-OlapR cells were treated with siCDK1 and subsequently treated with indicated doses of olaparib the following day. Cell viability was assessed 96 hours post olaparib treatment. **C.** LN-OlapR and 2B-OlapR were subjected to varying doses of BMS-265246 and response was assessed via cell viability assay 96 hours post treatment. **D.** LN-OlapR and 2B-OlapR cells were treated with either BMS-265246 or olaparib for 96 hours. Whole cell lysates were then prepared and subjected to western blot for indicated proteins. Tubulin served as a loading control. **E.** LN-OlapR and 2B-OlapR cells were treated with indicated doses of BMS-265246 +/− olaparib and cell viability was assessed 5 days post treatment. * = p-value ≤ 0.05 compared to all other samples.